# Heat and Moisture Advection over Antarctic Sea Ice

EDGAR L. ANDREAS

*U.S. Army Cold Regions Research and Engineering Laboratory, Hanover, NH 03755*

(Manuscript received 21 April 1984, in final form 18 December 1984)

ABSTRACT

Surface-level meteorological observations and upper-air soundings in the Weddell Sea provide the first *in situ* look at conditions over the deep Antarctic ice pack in the spring. The surface-level temperature and humidity were relatively high, and both were positively correlated with the northerly component of the 850 mb wind vector as far as 600 km from the ice edge. Since even at its maximum extent, at least 60% of the Antarctic ice pack is within 600 km of the open ocean, long-range atmospheric transport of heat and moisture from the ocean must play a key part in Antarctic sea ice heat and mass budgets. From one case study, the magnitude of the ocean's role is inferred: at this time of year the total turbulent surface heat loss can be 100 W $m^{-2}$ greater under southerly winds than under northerly ones.

## 1. Introduction

Because Antarctic sea ice has an annual cycle that ranges between a coverage of about $20 \times 10^6$ $km^2$ at maximum extent and only $3 \times 10^6$ $km^2$ at minimum extent, the surface energy fluxes in the Southern Ocean undergo similar large changes (e.g., Gordon, 1981). Presumably then, Antarctic sea ice plays an important role in the climate of the Southern Hemisphere; therefore, many have tried to relate sea ice conditions to climatic variables or to the atmospheric circulation around Antarctica. These studies fall into three general categories: analyses seeking correlations between sea ice and atmospheric variables without regard to cause and effect; analyses presupposing that the ice affects atmospheric circulation; and, conversely, analyses assuming that the atmosphere forces the sea ice. The fourth possibility, a feedback-coupled ice-atmosphere system, has received little attention.

Fletcher (1969) initiated the correlation-type studies. Using the scant data available before the satellite era, he found a positive correlation between ice coverage in Scotia Bay and the intensity of the zonal wind at New Zealand. Streten and Pike (1980) continued this line of research on a five-year record (1972–77) of satellite-derived ice extent. They, too, found a correlation between the mean zonally averaged westerlies and the latitude of the zonally averaged ice edge, and increasing variability in the westerlies correlated with increasing variability in the average ice extent.

Schwerdtfeger and Kachelhoffer (1973), Ackley and Keliher (1976), and Ackley (1981) took the perspective that changes in the sea ice cover were generally forcing the atmosphere. Schwerdtfeger and Kachelhoffer (1973) supported this view by showing significant correlation between ice extent and the frequency of occurrence of cyclonic vortices: the latitude band of maximum cyclone frequency seemingly moved south with the retreating ice, and frequency maxima occurred in the Weddell and Ross Seas, which Streten and Pike (1980) identified as the regions of greatest variability in ice extent. Ackley (1981) reiterated the theme that variability in the ice extent corresponded broadly with regions of high variability in the zonal wind. In each of these studies, cyclogenesis driven by the release of baroclinic instability near the ice margin—where the meridional temperature gradient was supposed to be strongest—was the postulated mechanism for observed correlations between cyclones and ice extent.

Taking the opposite viewpoint, Gordon and Taylor (1975) proposed that atmospheric forcing through Ekman divergence (e.g., Neumann and Pierson, 1966) could explain the relationship between cyclones and ice extent. A curl in the wind stress—a cyclonic vortex—causes a general divergence in the oceanic mixed layer: the ice spreads open, new ice forms, and the ice field consequently expands. Ackley and Keliher (1976), however, described a sea ice model that predicts that ice of "normal" concentration will converge rather than diverge under a cyclonic vortex.

Although recognizing that Antarctic sea ice both responds to and forces the atmosphere, Cavalieri and Parkinson (1981) and Parkinson and Cavalieri (1982) presented some persuasive evidence for another atmospheric explanation of cyclone-ice correlations. Figure 7 in Cavalieri and Parkinson (1981), also Fig. 2-9 in Zwally *et al.* (1983), shows the Weddell Sea ice edge advancing under the southerly wind west of a persistent low-pressure center; in their Fig. 11, the ice edge retreats under a northerly wind east of another persistent low. Though suggesting alternatives,

their analysis left the actual physics of advance or retreat unclear. Does a northerly wind carry enough oceanic heat to melt ice, while a cold, southerly wind forms it, or does a northerly wind compact it, while a southerly wind distends it? That is, is the forcing predominantly thermodynamic or dynamic? Hibler and Ackley (1983) showed that the dominant forcing depends on the season. On the basis of a numerical sea ice model with rudimentary ice-atmosphere feedback they found that, except in the western Weddell Sea, the ice advance is primarily thermodynamic, while the retreat depends on ice advection and the presence of leads and so is largely dynamic.

This study provides some additional information on the thermodynamic control of ice extent using data collected in the eastern Weddell Sea in October and November 1981 during a cruise on the Soviet icebreaker *Mikhail Somov* (Gordon, 1982). Records of surface-layer temperature and humidity and of upper-air winds show that in the spring a northerly wind can carry oceanic heat and moisture long distances over the sea ice; similarly, a southerly wind off the Antarctic continent remains cold and relatively dry as it traverses the ice. The direction of the geostrophic wind, therefore, has an important thermodynamic role—as well as a likely dynamic one—in the heat and mass budgets of Antarctic sea ice.

## 2. Observations

The *Somov* crossed the Antarctic ice edge at 56°15′S about midday on 20 October 1981. We worked in the ice until 14 November, penetrating into the "deep pack" (Ackley *et al.*, 1982) as far as 62°28′S—over 600 km from the ice edge (Fig. 1).

During this time we measured upper-air wind profiles at 0000 and 1200 GMT (also local time) using a Väisälä MicroCORA radiosonde system with RS21-12CN sondes (Andreas and Richter, 1982). Andreas (1983) tabulated all of these upper-air data. The MicroCORA system uses the Omega navaid signals to track the sonde; our wind speed measurements were accurate to better than 1 m $s^{-1}$ in this region of the Antarctic (Olson, 1979). The measured wind vector at 850 mb is used to represent the geostrophic flow; this level, generally 1000–1200 m, was always at or above the top of the atmospheric boundary layer (ABL).

These *in situ* measurements of the geostrophic flow are more reliable than winds estimated from the analysis fields for this data-poor area; Fig. 2 confirms this. The direction and speed of the measured 850 mb wind are compared in the figure with the geostrophic wind at the *Somov* estimated graphically from surface pressure charts. These charts were the 12-hourly Australian analysis fields provided by the National Climate Center, Asheville, North Carolina. Although the measured and estimated wind directions agree well, the estimated wind speed tends to overestimate the actual wind speed by about 50%. Hibler and Ackley (1983) also documented discrepancies between *in situ* measurements from the Weddell Sea and analysis field values; they inferred that these resulted because the Australian analysis ignores the presence of the sea ice (S. F. Ackley, personal communication, 1984).

The *Somov* cruise produced a high quality set of atmospheric surface-level temperature and humidity data. These humidity data, in particular, are the first accurate values ever measured over the deep Antarctic pack. Three identical General Eastern 1200MPS temperature and dew point monitoring systems were used for the measurements, each having its own aspirated radiation shield that houses both temperature and dew point sensors. The temperature sensor in each aspirator is a platinum resistance thermometer (PRT); the humidity sensor is a cooled-mirror dew point hygrometer, with a second PRT sensing the mirror temperature (the dew point). Both sensors have calibrations traceable to NBS standards. The calibration of each sensor was checked virtually every day; therefore, the accuracy of individual temperature and dew-point measurements was ±0.2°C at the temperatures that we encountered.

One temperature/humidity unit was mounted on a short boom on the bow of the *Somov;* the other two were set up side-by-side in a well exposed location on the (rear) helicopter deck; each was 11 m above the surface. Generally, all three instruments were in operation; the recorded observations were then the averages of the three temperature or dew point values. If one of the sensors was yielding spurious values, however, we could ignore it and still have two values for averaging. There was no evidence of systematic differences in either variable between the bow and helicopter deck locations.

Buck's (1981) method was used to convert dew point and temperature values to vapor pressures and standard methods were then applied to find specific and relative humidity. To make the temperature and humidity data compatible with the 12-hourly radiosonde data, 12-hourly averages at 0000 and 1200 GMT were computed by applying a triangular weighting function of 12-h base width to each data series.

## 3. Results

Figure 3 shows time series of ship distance south of the ice edge, the relative humidity (RH), the specific humidity ($Q$), the air temperature ($T$), and the northerly component of the measured 850 mb wind vector ($V_N$). The relative humidity was high—rarely did it fall below 75%. Andreas and Ackley (1982) had previously assumed—in the absence of

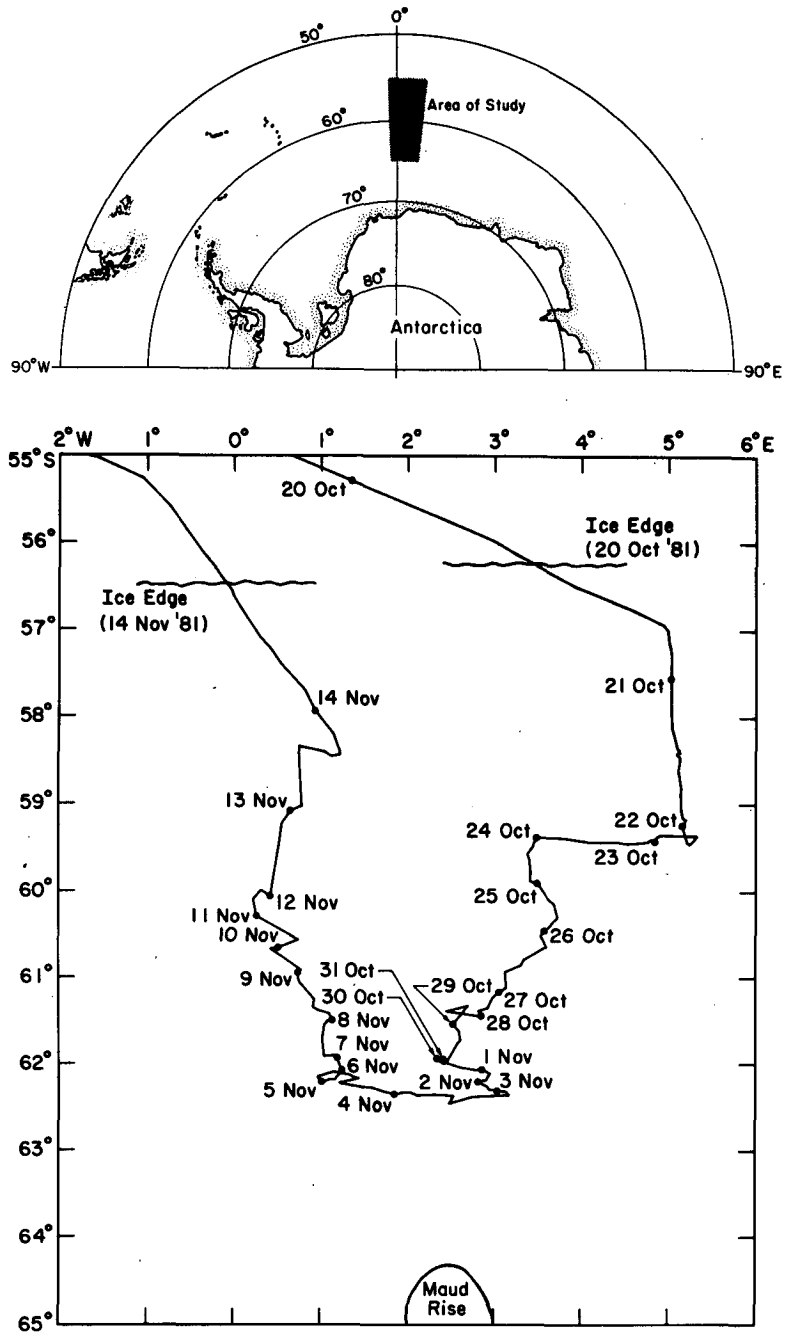


FIG. 1. Cruise track of the *Somov*. Dots mark the beginning of the indicated day.

reliable data—that the relative humidity in the Antarctic spring was approximately 60%. The air temperatures, though high by Arctic standards, seem compatible with the contour plots for this time of year as presented by Zwally *et al.* (1983). Their large contouring interval and monthly averaging, however, preclude a more meaningful comparison. No other *in situ* data are available for comparison.

Visual inspection of the time series suggests a source for the heat and moisture. Temperature and humidity are well correlated and each seems correlated with $V_N$; that is, a northerly wind—off the ocean—is relatively warm and moist; a southerly wind is cooler and drier. There is no suggestion, however, that the variables are correlated with distance from the ice edge. Wexler (1959) also observed the strong poleward

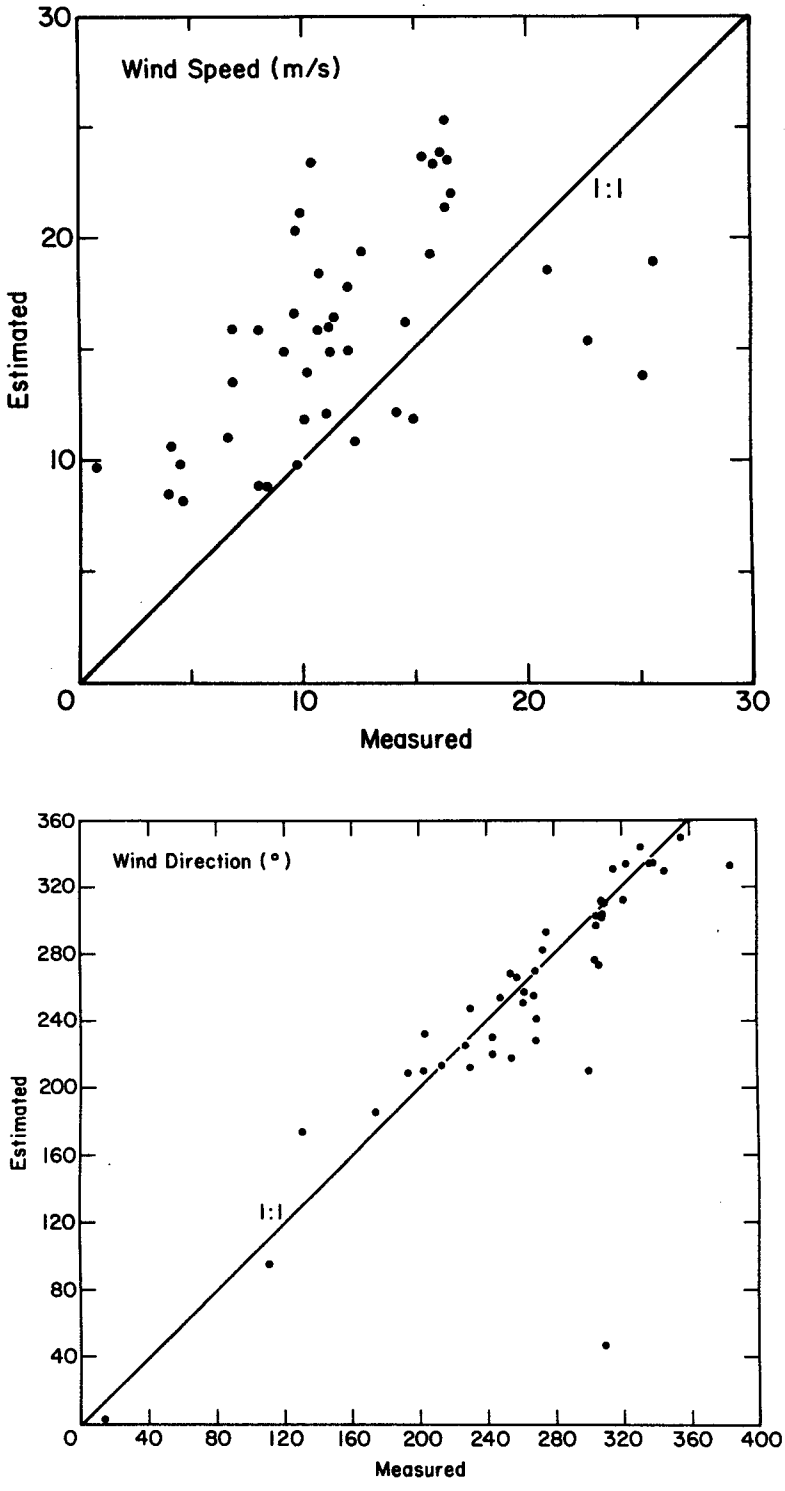


FIG. 2. Comparisons of the speed and direction of the measured 850 mb wind with estimates of the geostrophic wind obtained from surface pressure analysis fields.

advection of oceanic heat, even at the South Pole; but he found the heat there being carried higher in the troposphere rather than in the atmospheric boundary layer, as suggested here.

The cross-correlation functions of $T$, $Q$, and RH with $V_N$ in Fig. 4 substantiate the foregoing intuitive analysis. Both $T$ and $Q$ are correlated with $V_N$ with better than 99% confidence for lags from $-1$ day to

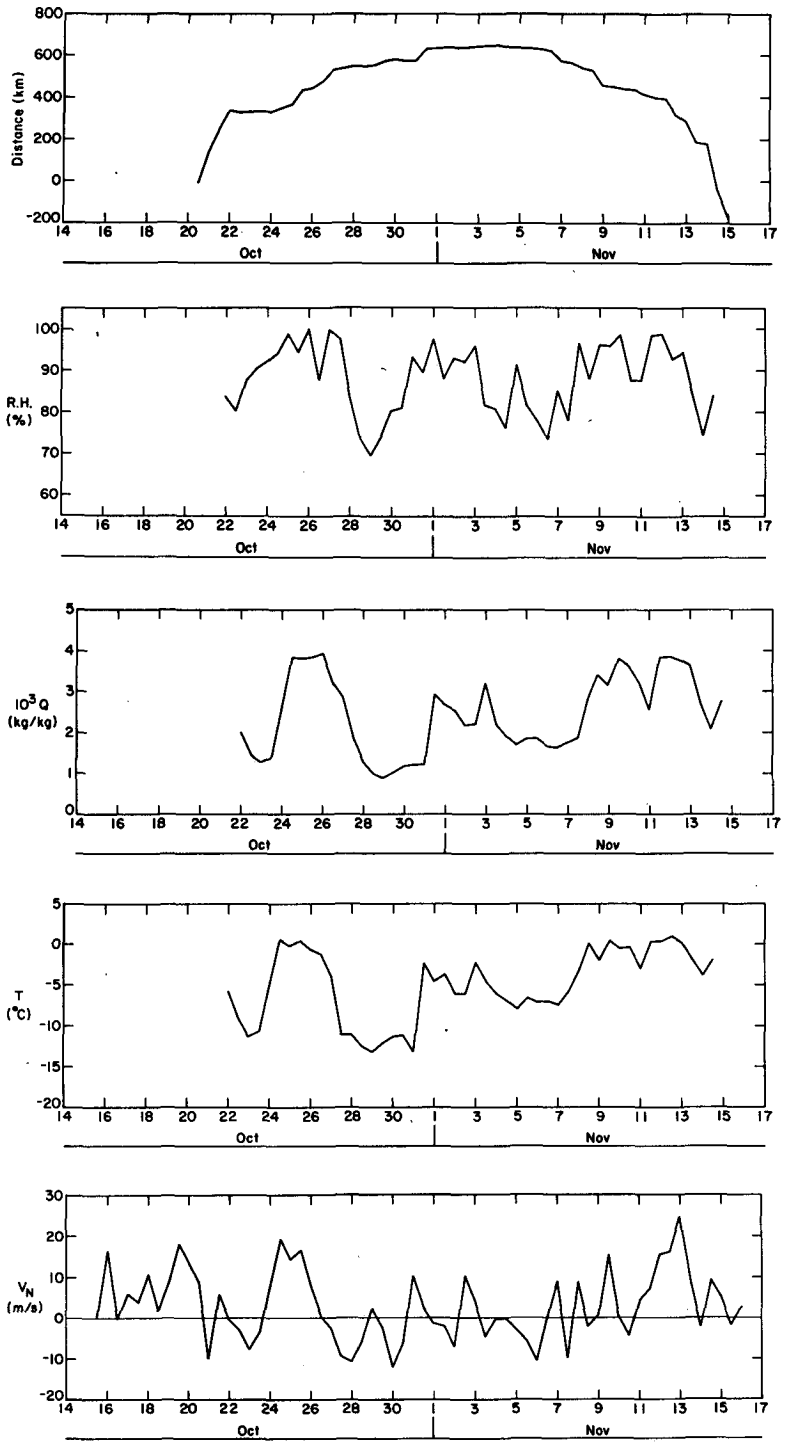


FIG. 3. Time series of the *Somov's* distance from the ice edge, the 12-h-averaged surface-level relative humidity, specific humidity, and temperature and individual radiosonde measurements of the northerly component of the 850 mb wind vector.

+½ day. Relative humidity is correlated with $V_N$ with better than 99% confidence at zero lags.

The details of the cross-correlation functions imply that the open ocean was a source for the heat and moisture. The $T$–$V_N$ and $Q$–$V_N$ cross-correlations have main peaks at −½ day; that is, $T$ and $Q$ are best correlated with $V_N$ when the wind time series measured at the *Somov* leads the local temperature

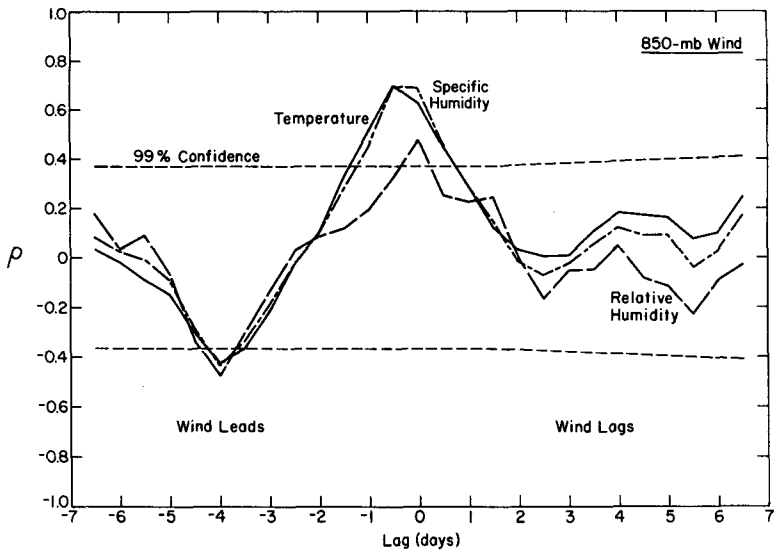


FIG. 4. Cross-correlation functions of temperature, specific humidity and relative humidity with $V_N$. Dashed lines delimit the 99% confidence interval.

and specific humidity time series by 12 hours. Note that an air mass moving at 10 m $s^{-1}$ (typical of the 850 mb wind) can cover 430 km in 12 h, roughly our distance from the ice edge. The 12-h averaging of the scalar series effectively extends this distance to 650 km. Thus, the location of the maxima in the $T$–$V_N$ and $Q$–$V_N$ cross-correlations suggests that atmospheric transport of oceanic heat and moisture produced the high temperature and specific humidity events seen at the ship. The width of these main cross-correlation peaks, 1.5 days, is an indicator of the temporal variability within the ABL.

The RH–$V_N$ cross-correlation is different than the $T$ and $Q$ cross-correlations: it has a lower main peak and significant correlation only at zero lags. Evidently, relative humidity behaves differently than specific humidity over sea ice. Specific humidity is a measure of how much water vapor the air holds and, therefore, has a strong temperature dependence. A warm air mass can hold much more water vapor than a cold air mass—hence the similarity between the $T$ and $Q$ time series and the $T$–$V_N$ and $Q$–$V_N$ cross-correlation functions. On the other hand, relative humidity, which is the ratio of actual water vapor content to potential water vapor content, is largely independent of temperature. Throughout most of the year, the deep Antarctic ice pack undergoes surface ablation. The ablation rate depends strongly on wind speed. An increase in the local wind speed will, thus, generally cause an increase in the relative humidity, regardless of wind direction. Consequently, the relative humidity should be high when $|V_N|$ is large (not just when $V_N$ is large) and lower when $|V_N|$ is small. In other words, this effect tends to produce a good, positive correlation between RH and $V_N$ when $V_N$ is large and positive but a good, negative correlation when $V_N$ is large and negative. It thus confounds the RH–$V_N$ cross-correlation function at zero lags and explains why RH is not as well correlated with $V_N$ as $T$ and $Q$.

Another effect, however, is evidently strong enough to give the significant correlation between RH and $V_N$ at zero lags. An oceanic air mass moving south across the sea ice would be cooled; its saturation vapor pressure would consequently decrease. Even without a change in its moisture content, its relative humidity would therefore increase. Conversely, a continental air mass moving north across the sea ice would warm, and its saturation vapor pressure would increase. With no change in its specific humidity, its relative humidity would decrease. Thus, simple physics leads to an inherent correlation between RH and $V_N$.

Recognizing these opposing effects of local wind speed changes and the meridional temperature gradient, we can infer what causes the significant main peak in the RH–$V_N$ cross-correlation function. Long-range atmospheric transport of water vapor and the attendant effects of the meridional temperature gradient must have been responsible for the significant cross-correlation. The main cross-correlation peak is significant only at zero lags because the relative humidity also responds immediately to changes in the local surface wind. This effect, however, did not destroy the peak entirely because the strongest winds were northerly ($V_N$ positive, see Fig. 3).

The significant negative peak at a lag of −4 days in all of the cross-correlation functions in Fig. 4 reflects the time scale of the atmospheric systems the *Somov* encountered. That is, a lag of −4 days correlates the low temperature and humidity associated with the southerly wind on the back side of a passing low with the positive $V_N$ on its front side.

Since the 850-mb wind is not always available, the

foregoing analysis was redone using 12 hourly averages (again, triangular weighting function) of the northerly component of the surface wind measured on the *Somov* ($V_{Ns}$). With the fairly small turning angle over sea ice (Brown, 1981; Thorndike and Colony, 1982), $V_{Ns}$, not surprisingly, is well correlated with $V_N$. Figure 5 shows that a linear dependence on $V_N$ would explain over 70% of the variance of $V_{Ns}$. The width of the cross-correlation peak, 1.5 days, again reflects the temporal variability of the atmospheric boundary layer.

The cross-correlation functions of $T$, $Q$, and RH with $V_{Ns}$ in Fig. 6 look much like those in Fig. 4. Again, the $T$–$V_{Ns}$ and $Q$–$V_{Ns}$ correlations have main peaks at a lag of −½ day. Both correlation coefficients, however, are slighty higher here than in Fig. 4—probably a result of the enhanced $V_{Ns}$ values resulting from clockwise turning of the wind profile under geostrophic winds predominantly from the northwest. The width of the $T$ and $Q$ peaks, 2–2½ days, is similar to the peak widths in Fig. 4 and, therefore, emphasizes the time scale of the temporal variability over Antarctic sea ice.

The cross-correlation function of relative humidity with $V_{Ns}$ shown in Fig. 6 is strikingly similar to the RH–$V_N$ function in Fig. 4. This similarity undercores the importance of local wind events on the relative humidity.

Although RH is significantly correlated with $V_{Ns}$ at a lag of −4 days, this is not so for either $T$ or $Q$. This is somewhat puzzling. Since $V_N$ and $V_{Ns}$ are uncorrelated at a lag of −4 days, it is not surprising that $T$ and $Q$ are uncorrelated with $V_{Ns}$ there, although both were correlated there with $V_N$. I can suppose only that the RH–$V_{Ns}$ correlation at −4 days is a combination of the very high $V_{Ns}$–$V_N$ correlation at zero lags and the good (negative) RH–$V_N$ correlation at −4 days.

## 4. Discussion

Though short, our time series imply that thermodynamic processes explain, in part, the observed correlations between Antarctic sea ice extent and atmospheric indices, at least in the spring. A northerly wind can carry oceanic heat deep into the pack, while a southerly wind can cool and dry the atmosphere over a large area of the pack ice. Thermodynamic processes at the ice surface are thus strongly coupled to the geostrophic wind direction. Freeze and thaw cycles or advance and retreat periods may thus be episodic, especially in the spring and fall when the energy budget of the ice is nearly balanced (Gordon, 1981). Andreas *et al.* (1984) also pointed out this probable episodic behavior of advance and retreat periods nearer the ice edge.

It is fairly easy to see that if the geostrophic wind has a long open ocean fetch, it is indeed oceanically derived heat and moisture that we are seeing 600 km into the ice. Admittedly, the concentration of Antarctic sea ice is low by Arctic standards; the open water could thus serve as a heat and moisture source under the right conditions. A northerly wind in initial equilibrium with the open ocean, however, does not present the right conditions. The open water percentage decreases poleward with distance from the ice edge (Zwally *et al.*, 1983); the surface must also cool with distance. An air mass crossing the ice edge and moving southward could in no way be warmed or

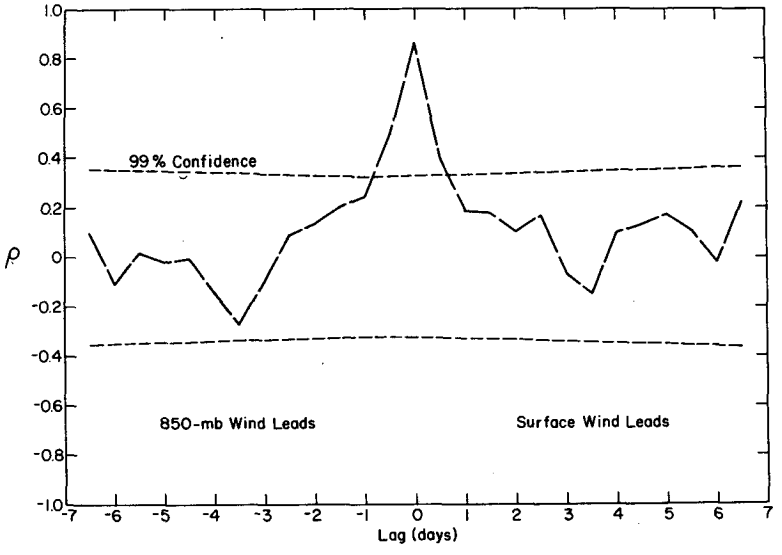


FIG. 5. Cross-correlation function of the 12-h-averaged northerly component of the surface wind vector with the northerly component of the 850 mb wind vector. Dashed lines delimit the 99% confidence limit.

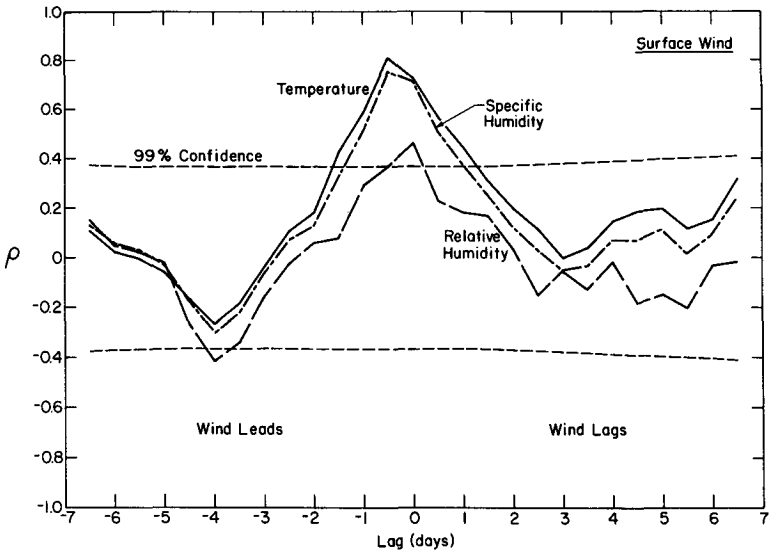


FIG. 6. As in Fig. 4, but for temperature, specific humidity and relative humidity with $V_{N5}$. Dashed lines delimit the 99% confidence interval.

moistened above its oceanic equilibrium. It would, in fact, cool and dry if the meridional temperature gradient at the ice surface were strong enough. Our observations that the temperature and humidity remain surprisingly high under northerly winds, even 600 km from the ice edge, suggest that the temperature gradient is rather weak in the spring. Andreas *et al.* (1984) made the same observation in the Antarctic marginal ice zone; in their study the surface-layer air temperature under a northerly wind decreased only about 1°C along a 150 km path over sea ice of concentrations up to 80%. The many leads and polynyas evidently prevent the ice surface from being cooled much more than 10°C below freezing at this time of year, even under a southerly wind.

To appreciate the magnitude of the surface flux difference between northerly and southerly winds, let us look at the conditions from 25–31 October. The Fig. 3 time series show a southerly wind event from 27–31 October that produced the lowest temperatures and humidities we encountered during the cruise. In contrast, the 850 mb wind during the preceding two days had a strong northerly component, and both temperature and humidity were high. Let us put this event in a synoptic context and then compute representative turbulent surface fluxes during the event.

Although surface pressure analysis fields for the Southern Ocean are sometimes untrustworthy, let us, at least qualitatively, assess the synoptic conditions from 25–31 October 1981 (see Fig. 7). These maps are again the Australian analysis fields from the National Climate Center.

At noon on 25 October the *Somov* was just east of a deep low; the geostrophic wind was, thus, northerly and had a significant oceanic fetch. Figure 3 confirms the northerly wind and shows that temperature and humidity were both relatively high. During the next two days the low passed directly over us, so at noon on 27 October we were to its west; the geostrophic wind at the *Somov* was consequently from the south. The RH, $Q$, $T$, and $V_N$ time series in Fig. 3 all show the consequences of the passage; the 850 mb wind swung to the south, and the temperature and humidity fell precipitously.

During the next two days another low pressure center moved into our area, but it stayed somewhat to the north; Fig. 7 shows the surface pressures at noon on 29 October. This northerly low produced a weak southeasterly wind at the *Somov;* $V_N$ in Fig. 3 is thus near zero, but $T$, $Q$, and RH remain low. Evidently, the air mass was of continental rather than oceanic origin or had followed a very long path over sea ice. As the low moved to the southeast, the southerly winds behind it kept the temperature and humidity low at the *Somov* for another day (Fig. 3). Finally, yet another low approached from the west and—since it was at roughly the latitude of the *Somov*—brought northerly winds, higher temperatures, and moist air from the ocean to our region. Figure 7 shows the synoptic situation at noon on 31 October, while Fig. 3 reflects the sequence of changes associated with the approaching low that finally ended the low temperature event.

Estimates of the surface sensible and latent heat fluxes before, during, and after this event confirm the influence of the geostrophic wind direction on the surface energy budget. A simple flux-gradient iteration procedure (described by Andreas *et al.,* 1984) was used for these estimates; the data consisted of shipboard observations of wind speed and surface temperature, along with the temperature and specific humidity values shown in Fig. 3. Table 1 summarizes

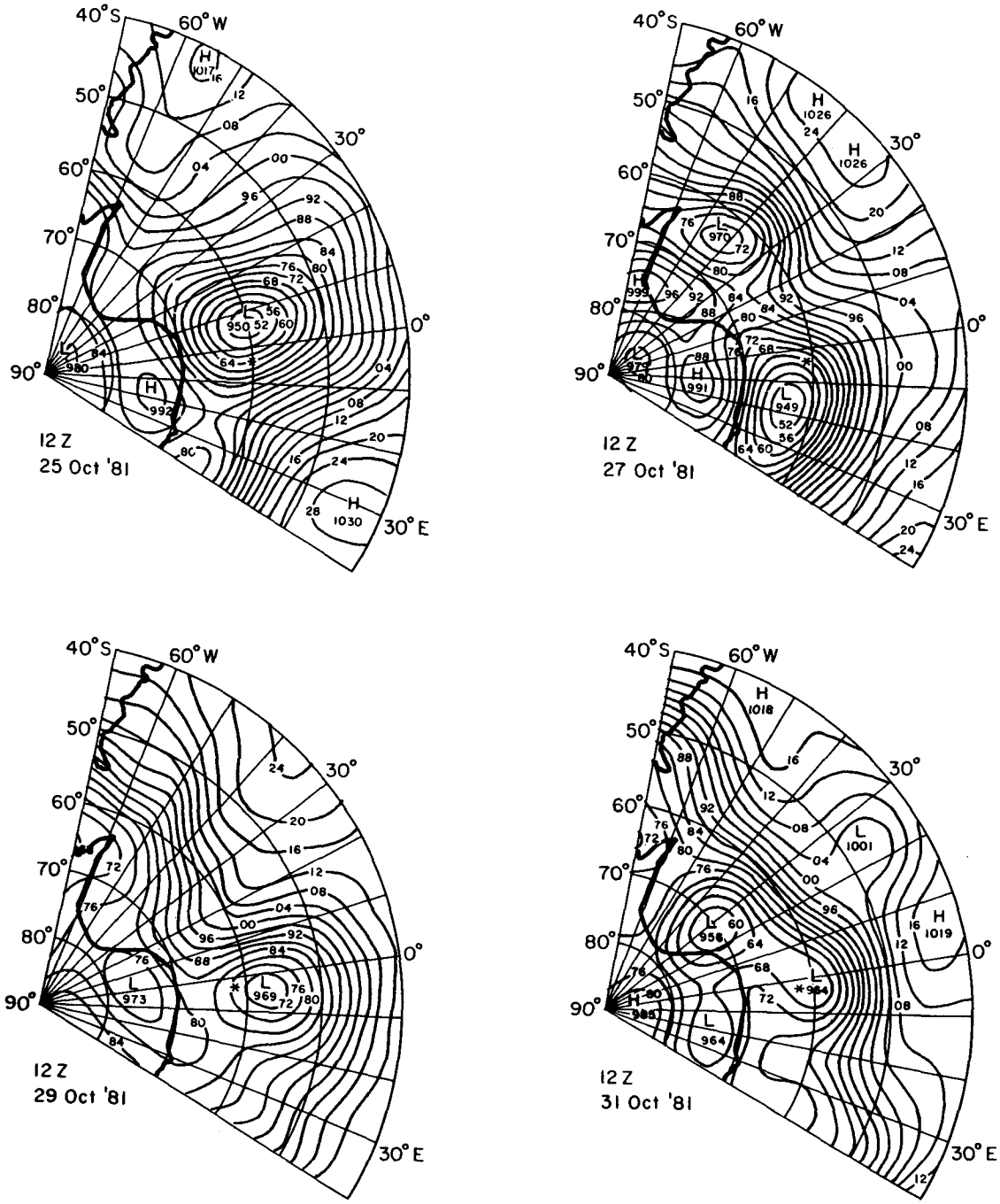


FIG. 7. Sea-level pressure fields during the low temperature event of 27–31 October 1981. The star near the 0° meridian shows location of the *Somov*.

the relevant observations and the associated fluxes for the four cases represented by the maps in Fig. 7.

The fluxes in Table 1 clearly depend on whether the air mass at our location was continental or oceanic but are unrelated to distance from the ice edge. Before the low temperature event on 25 October and after it on 31 October, the oceanic heat and moisture carried in on northerly winds kept the surface-layer air near thermal equilibrium with the surface. Sensible and latent heat losses from the surface were thus minimal—in fact, on 31 October, 630 km from the ice edge, the air was transferring heat to the surface. Since the net radiation budget was negative on both 25 and 31 October, there was likely some melting on these days. On 27 and 29 October, however, when the air mass was probably

TABLE 1. Data and results of a flux-gradient estimate of the turbulent sensible and latent heat fluxes (Time GMT).*

| | 25 Oct 1981 1200 | 27 Oct 1981 1200 | 29 Oct 1981 1200 | 31 Oct 1981 1200 |
|---|---|---|---|---|
| Distance (km) | 430 | 540 | 570 | 630 |
| $U$ (m s$^{-1}$) | 9.0 | 12.0 | 10.0 | 8.0 |
| $T$ (°C) | −0.2 | −11.1 | −12.1 | −2.3 |
| $T_s$ (°C) | 0.0 | −3.5 | −8.9 | −3.6 |
| $Q$ ($10^{-3}$ kg/kg) | 3.85 | 1.53 | 1.02 | 2.94 |
| $Q_s$ ($10^{-3}$ kg/kg) | 3.96 | 2.97 | 1.83 | 2.94 |
| $u_*$ (m s$^{-1}$) | 0.31 | 0.45 | 0.36 | 0.24 |
| $H_s$ (W m$^{-2}$) | 2 | 169 | 58 | −15 |
| $H_L$ (W m$^{-2}$) | 5 | 84 | 40 | 0 |
| $R_n$ (W m$^{-2}$) | −45 | −110 | −140 | −380 |

*$U$ = the wind speed at a reference height of 21 m; $T$ and $Q$ = temperature and specific humidity at 11 m; $T_s$ and $Q_s$ = the temperature and specific humidity at the surface; $u_*$ = the computed friction velocity; $H_s$ and $H_L$ = the computed sensible and latent heat fluxes; $R_n$ = the measured net radiation (see Andreas and Makshtas, 1983). Positive fluxes indicate a transfer of heat from the surface to the atmosphere.

of continental origin, the turbulent surface heat losses were large. These losses overwhelmed the radiative fluxes on 27 October and probably fostered ice formation. Ackley and Smith (1983) observed extensive areas of grease ice on this day, substantiating this heat budget analysis. By 29 October the ice surface had cooled under the persistent cold winds; the turbulent heat losses consequently decreased though the winds were of similar strength. Adding a constant oceanic conductive heat flux $C$ of 20–25 W m$^{-2}$ (Gordon *et al.*, 1984) into the surface energy budget, we see that the ice was probably warming or melting on that day, even with the low temperatures (i.e., $R_n - C + H_s + H_L \approx -60$ W m$^{-2}$). However, the cold continental air kept this to a minimum, despite the large shortwave flux to the surface.

Although it is always dangerous to extrapolate from the specific to the general, these flux computations at least suggest an order of magnitude for the difference in the total turbulent surface flux between northerly and southerly winds. In the spring a southerly wind removes roughly 100 W m$^{-2}$ more heat from the surface than a northerly wind. Or, expressed in another way, a northerly wind makes a −100 W m$^{-2}$ difference in the surface energy budget. A flux to the surface, constant at 100 W m$^{-2}$, can melt 3 cm of ice per day.

The time series in Fig. 3 show no dramatic decrease in temperature or humidity as our distance from the ice edge increased from 200 to 600 km. Hence, a northerly wind off the ocean can influence the surface-layer temperature and humidity fields for distances of at least 600 km from the ice edge; i.e., even at maximum ice extent, marine air can reach roughly 60% of the Antarctic ice pack. At minimum ice extent, it can reach virtually the entire pack. Contrast this with conditions in the Arctic Ocean, which has only a very limited open ocean boundary.

## 5. Conclusions

The temperature and humidity time series presented herein are the first reliable, *in situ* measurements from the deep Antarctic ice pack during its near-maximum extent. Their main lessons are the temporal variability of both fields and the relatively mild conditions over the deep pack in the spring. The correlations of temperature and humidity with meridional wind imply an important thermodynamic contribution to previously observed relationships between sea ice extent and synoptic-scale atmospheric variables. They do not, however, rule out a concomitant dynamic contribution from the meridional wind stress. This may be as important as the thermodynamics in controlling ice extent, but the data are insufficient to investigate it.

The results also have implications for modeling both sea ice and the atmospheric boundary layer in the Antarctic. Monthly mean geostrophic winds (e.g., Parkinson and Washington, 1979) are not adequate for driving sea ice models. The day-to-day variability of the wind leads to episodic behavior in the surface energy budget. Atmospheric forcing fields updated daily (e.g., Hibler and Ackley, 1983) would seem to be a minimum requirement.

Because a northerly wind can still be losing heat 600 km from the ice edge, and because a southerly wind crossing the continental boundary immediately begins extracting heat and moisture from open water areas within the sea ice, the ABL over Antarctic sea ice is rarely in equilibrium with the surface. Modeling it will consequently be a large-scale boundary layer modification problem; one-dimensional models, which are successful in the Arctic, would be hard to defend here.

*Acknowledgments.* Stanislav Bobrov and Valerii Posazhenikov of the Arctic and Antarctic Research Institute, Leningrad, made all of the MicroCORA soundings; Brett Murphy helped with the computations; and William Bates drafted the figures. My colleagues, Steve Ackley and Tony Gow, offered helpful comments on an early draft of the manuscript; Mark Hardenberg provided editorial assistance. Two anonymous reviewers spent a lot of time with the manuscript and suggested many improvements. The National Science Foundation supported this research through Grants DPP 80-06922 and DPP 81-20024. The National Oceanic and Atmospheric Administration, Office of Special Research and Programs, provided funds for the lease of the MicroCORA through the National Science Foundation, Grant DPP 82-03489.

## REFERENCES

Ackley, S. F., 1981: A review of sea-ice weather relationships in the Southern Hemisphere. *Sea Level, Ice, and Climate Change*, I. Allison, Ed., IAHS Publ. **131**, 127–159. [International

Association of Hydrological Sciences, 2000 Florida Ave. NW, Washington, DC 20009.]

——, and T. E. Keliher, 1976: Antarctic sea ice dynamics and its possible climatic effects. *AIDJEX Bull.*, **33,** 53–76. [Arctic Ice Dynamics Joint Experiment, Div. Marine Resources, University of Washington, Seattle, Wash. 98105.]

——, and S. J. Smith, 1983: Reports of the U.S.-U.S.S.R. Weddell Polynya Expedition, October–November 1981: Vol. 5, Sea ice observations. Special Rept. 83-2, U.S. Army Cold Regions Research and Engineering Laboratory, Hanover, N.H., 59 pp. [NTIS: AD-A130 140/7.]

——, —— and D. B. Clarke, 1982: Observations of pack ice properties in the Weddell Sea. *Antarct. J. U.S.*, **17,** 105–106.

Andreas, E. L., 1983: Reports of the U.S.-U.S.S.R. Weddell Polynya Expedition, October–November 1981: Vol. 6, Upper-air data. Special Rept. 83-13, U.S. Army Cold Regions Research and Engineering Laboratory, Hanover, N.H., 288 pp. [NTIS: AD-A134 871/3.]

——, and S. F. Ackley, 1982: On the differences in ablation seasons of Arctic and Antarctic sea ice. *J. Atmos. Sci.*, **39,** 440–447.

——, and W. A. Richter, 1982: An evaluation of Vaisala's MicroCORA Automatic Sounding System. CRREL Rept. 82-28, U.S. Army Cold Regions Research and Engineering Laboratory, Hanover, N.H., 17 pp. [NTIS: AD-B070 011/L.]

——, A. P. Makshtas, 1983: Reports of the U.S.-U.S.S.R. Weddell Polynya Expedition, October–November 1981: Vol. 7, Surface-level meteorological data. Special Rept. 83-14, U.S. Army Cold Regions Research and Engineering Laboratory, Hanover, N.H., 32 pp. [NTIS: AD-A134 476/1.]

——, W. B. Tucker III and S. F. Ackley, 1984: Atmospheric boundary-layer modification, drag coefficient, and surface heat flux in the Antarctic marginal ice zone. *J. Geophys. Res.*, **89,** 649–661.

Brown, R. A., 1981: Modeling the geostrophic drag coefficient for AIDJEX. *J. Geophys. Res.*, **86,** 1989–1994.

Buck, A. L., 1981: New equations for computing vapor pressure and enhancement factor. *J. Appl. Meteor.*, **20,** 1527–1532.

Cavalieri, D. J., and C. L. Parkinson, 1981: Large-scale variations in observed Antarctic sea ice extent and associated atmospheric circulation. *Mon. Wea. Rev.*, **109,** 2323–2336.

Fletcher, J. O., 1969: Ice extent on the Southern Ocean and its relation to world climate. RM-5793-NSF, Rand Corporation, 108 pp. [1700 Main St., Santa Monica, Calif. 90406.]

Gordon, A. L., 1981: Seasonality of Southern Ocean sea ice. *J. Geophys. Res.*, **86,** 4193–4197.

——, 1982: The U.S.-U.S.S.R. Weddell Polynya Expedition. *Antarctic J. U.S.*, **17,** 96–98.

——, and H. W. Taylor, 1975: Seasonal change of Antarctic sea ice cover. *Science,* 187, 346–347.

——, C.T.A. Chen and W. G. Metcalf, 1984: Winter mixed layer entrainment of Weddell Deep Water. *J. Geophys. Res.*, **89,** 637–640.

Hibler, W. D., III, and S. F. Ackley, 1983: Numerical simulation of the Weddell Sea pack ice. *J. Geophys. Res.*, **88,** 2873–2887.

Neumann, G., and W. J. Pierson, Jr., 1966: *Principles of Physical Oceanography.* Prentice-Hall, Englewood Cliffs, N.J., 545 pp.

Olson, M. L., 1979: Global accuracy of Omega-derived winds. *Atmos. Technology,* **10,** 14–23. [National Center for Atmospheric Research, P.O. Box 3000, Boulder, Colo. 80307.]

Parkinson, C. L., and W. M. Washington, 1979: A large-scale numerical model of sea ice. *J. Geophys. Res.*, **84,** 311–337.

——, and D. J. Cavalieri, 1982: Interannual sea-ice variations and sea-ice atmosphere interactions in the Southern Ocean, 1973–1975. *Ann. Glaciol.*, **3,** 249–254. [International Glaciological Society, Cambridge CB2 1ER, England.]

Schwerdtfeger, W., and St. Kachelhoffer, 1973: The frequency of cyclonic vortices over the Southern Ocean in relation to the extension of the pack ice belt. *Antarctic J. U.S.*, **8,** 234.

Streten, N. A., and D. J. Pike, 1980: Characteristics of the broadscale Antarctic sea ice extent and the associated atmospheric circulation 1972–1977. *Arch. Meteor. Geophys. Bioklim.*, **A29,** 279–299.

Thorndike, A. S., and R. Colony, 1982: Sea ice motion in response to geostrophic winds. *J. Geophys. Res.*, **87,** 5845–5852.

Wexler, H., 1959: Seasonal and other temperature changes in the Antarctic atmosphere. *Quart. J. Roy. Meteor. Soc.*, **85,** 196–208.

Zwally, H. J., J. C. Comiso, C. L. Parkinson, W. J. Campbell, F. D. Carsey and P. Gloersen, 1983: *Antarctic Sea Ice, 1973–1976: Satellite Passive-Microwave Observations.* NASA SP-459, National Aeronautics and Space Administration, Goddard Space Flight Center, Greenbelt, Md., 206 pp. [U.S. Government Printing Office, Washington, DC 20402.]